

Thermal, Morphological and Structural Characterization of Chitosan-Modified Hybrid Materials for Prosthodontics

AGRIPINA ZAHARIA^{1*}, VIORICA PLESCAN GHISMAN², CORINA LAURA STEFANESCU¹, VIORICA MUSAT^{2*}

¹ Ovidius University of Constanta, Faculty of Dentistry, 7 Ilarie Voronca Str., 900684, Constanta, Romania

² Dunarea de Jos University of Galati, Faculty of Engineering, Department of Materials Science and Engineering, Centre of Nanostructures and Functional Materials-CNMF, 47 Domneasca Str., 800008, Galati, Romania

The paper presents the thermal behavior of some hybrid materials for application in prosthodontics based on acrylic copolymers matrix with added chitosan. Chitosan is a plentiful natural biopolymer with excellent film-forming ability having the advantages of antimicrobial activity, biocompatibility and biodegradability. The effects of chitosan concentration and different modalities of its addition during the material preparation were investigated by modulated thermogravimetry (mTGA) and derivative scanning calorimetry (mDSC). The mTGA and mDSC techniques coupled with Tzero technique were used to investigate also the separation of the reversible (phase transition) and the non-reversible (chemical conversion) processes from the total heat flow and to calculate the kinetic parameters, respectively. Fourier transform infrared (FTIR) spectroscopy and scanning electron microscopy (SEM) data complete this study on the obtained hybrid biocompatible materials.

Keywords: acrylic copolymer, chitosan, hybrid biocompatible materials, modulated thermogravimetric analysis, modulated derivative scanning calorimetry

Polymethyl methacrylate (PMMA), also known as Plexiglas, is the most commonly used as denture plastic material due to relatively good mechanical properties and biocompatibility with the oral environment, as well as superiority to other materials in terms of manipulation, aesthetics and low cost [1]. PMMA is one of the hardest thermoplastics with high Young's modulus and low elongation at break, resistant on rupture and highly scratch resistant. The limit temperature of thermal stability of standard PMMA is only 65 °C, but heat stabilized derivatives can withstand to temperatures up to 100 °C and as low as -70 °C [2].

Mechanical properties and biological compatibility of PMMA can be improved by grafting natural polymers like chitosan which has the advantages of antimicrobial and tissue regenerative properties that are very important for prosthodontics [1, 3-10]. Chitosan is a plentiful natural biopolymer, whose degradation products are non-toxic, non-immunogenic and non-carcinogenic, and is more and more used by biomedical and pharmaceutical industries [11-13]. The use of acrylic-based self-polymerizing resin for the fabrication of temporary crowns and temporal seal of inlay cavities usually leads to direct chemical and biological effects on dental pulp tissue. In the same time, in the biological medium, the accumulation of microorganism deposit attached to the denture surface causes an inflammation known as denture stomatitis [14].

This paper presents some structural and morphological aspects, along with the thermal behavior of hybrid materials based on a commercial acrylic polymer matrix modified with chitosan, aiming to improve their biocompatibility and antimicrobial activity. The effect of chitosan was investigated by Fourier transform infrared spectroscopy (FTIR) for structure, by scanning electron microscopy (SEM) for morphology and by modulated thermogravimetry analysis (mTGA) and modulated derivative scanning calorimetry (mDSC) for thermal behaviour.

Experimental part

Materials and samples preparation

The as raw materials used for the preparation of the investigated samples were Duracryl® Plus (powder and liquid) produced by Spofa Dental (Czech Republic), chitosan with low-molecular-weight (50 kDa) and 75–85% degree of deacetylation purchased from Sigma–Aldrich and glacial acetic acid purchased from Beker.

The acrylic resin matrix was prepared by mixing the Duracryl powder (P) and liquid (L) components in the weight ratios of 2.5 : 1.0 or 2.5 : 0.5 (2.5 parts of powder and 1.0 or 0.5 parts of liquid) (table 1). The powder was poured into the liquid and mixed for 15 seconds at room temperature. The chitosan (1 g) has been dissolved in 50 mL acetic acid (1%) under magnetic stirring for 24 h. Two series of hybrid samples were prepared by adding the chitosan (Cs) in different proportions in relation to the Duracryl powder (P) and Duracryl liquid (L), after (Ac1-1 to Ac1-3 samples) or before (Ac2-1 to Ac2-3 samples) mixing the Duracryl powder with the Duracryl liquid (table 1). The resulting samples were exposed for 10 min at UV radiation ($\lambda = 254$ nm).

Materials characterization

The thermal behaviour of the raw materials and as-obtained hybrid material samples was investigated by modulated thermogravimetric (mTGA) and modulated dynamic scanning calorimetry (mDSC) coupled with Tzero techniques by using TGA Q5000 and DSC Q50 equipments from TA Instruments. The measurements were performed under synthetic air atmosphere (gas flow 25 mL/min), in the temperature range of 25–600 °C, at a heating rate of 10 °C/min. The modulated thermal regime was realised by superimposing a sinusoidal temperature modulation on the traditional underlying heating profile. Samples about 6 mg for mTGA and 4 mg for mDSC were used for recording the experimental curves.

* email: agrizaharia@yahoo.com, viorica.musat@ugal.ro

Table 1
PREPARATION OF THE INVESTIGATED SAMPLES

No. crt.	Sample symbol	Reactants addition order	Reagents ratio (L):(P):(Cs)	Type of material
1	Ac0	(L)+(P)	1.0: 2.5:0.0	Acrylic resin matrix
2	Ac1-1	(L+P)/(Cs)	1.0: 2.5:0.5	Hybrid materials (First series)
3	Ac1-2		1.0: 2.5: 1.0	
4	Ac1-3		0.5: 2.5:0.5	
5	Ac2-1	(Cs+P)/(L)	1.0: 2.5: 0.5	Hybrid materials (Second series)
6	Ac2-2		1.0: 2.5: 1.0	
7	Ac2-3		0.5: 2.5:0.5	

Fourier transform infrared (FTIR) spectra of pure chitosan, commercially Duracryl® Plus powder, acrylic matrix and hybrid acrylic-chitosan samples were recorded in the range between 4000 and 500 cm^{-1} with a NICOLET IS50 Advanced FTIR spectrometer (from Thermo Scientific) using attenuated total reflectance (ATR) on a ZnSe crystal.

The morphology of the hybrid samples was examined by scanning electron microscopy (SEM) using a FEI Q 200 microscope, in low vacuum conditions. Before examination, the samples were coated with a 4-5 nm thick conducting layer of Au using a SPI-Module™ sputter coater system.

Results and discussions

Structural and morphological characterization

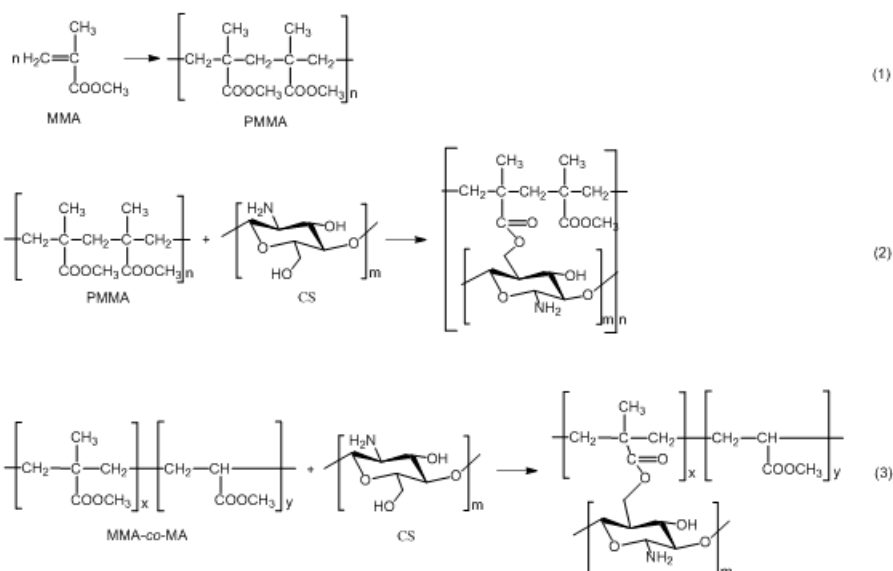
Duracryl® Plus powder consists in microspheres of >95% methylmethacrylate - methylacrylate (MMA-co-MA) copolymer and 1-5% dibenzoyl peroxide (DBP), while the liquid consists in 85-90% methylmethacrylate (MMA) and < 5% dimethyl-paratoluidine (DMPT) [15]. When the microspheres are introduced into the liquid, at the contact with the BDP polymerization initiator agent the MMA monomer polymerizes and forms a transparent solid film of PMMA, according to chemical reaction (1) (scheme 1). During formation of a cross-linked composite consolidated material, the MMA-co-MA microspheres are included.

While acryl monomers have C=C double bonds and methoxy groups (-OCH₃), which may interact among themselves or with other reactants by polymerization (chemical reaction 1, scheme 1) and/or condensation, respectively, the PMMA and MMA-co-MA polymers have only methoxy reactive groups that can lead to condensation reactions (chemical reactions 2 and 3, scheme 1). Chitosan has two types of reactive groups that can be used in the grafting. The chemical modification of chitosan molecules usually occurs at three reactive

positions: at the free amino groups at the C2 on deacetylated units and at the hydroxyl groups on the C3 and C6 carbons on acetylated or deacetylated units [8,16]. This allows grafting of different molecules to chitosan via strong covalent bonds, with the formation of functional derivatives. The chitosan grafting can be done with acrylic monomers by copolymerization reactions [17, 18] and with acrylic polymers by polycondensation reactions.

The attenuated total reflectance (ATR) FTIR spectra of the acrylic matrix (Ac0) and the hybrid materials resulted by adding chitosan to this matrix (samples Ac1-1 to A1-3 and A2-1 to A2-3) are shown in figure 1. The strong -C=O stretching band observed at 1720 cm^{-1} together with the $\times\text{C}\times\text{O}$ stretching vibrations of esters (C-C(=O), -O and O-C-C) at 1235 and 1132 cm^{-1} as well as the methyl and methylene -C-H stretchings and bendings at 2954 and 1430 cm^{-1} , respectively, reveals the characteristic absorption bands of poly(methyl methacrylate) both in the matrix (Ac0) and the obtained hybrid materials [19].

Many papers report that the chitosan molecules can be attached successfully to the PMMA surface by covalent bonding between the amine groups of chitosan and carboxylic groups of PMMA [3-8]. Some literature data state that the PMMA grafting of the chitosan is achieved through the condensation reaction of the carboxylic groups of PMMA with the amino (-NH₂) groups of chitosan and an amide is formed [20]. The FTIR spectra of the prepared samples presented in figure 1 suggest that, in the conditions of our study, the interaction between chitosan and acrylic polymer would have been achieved only through a transesterification reaction of the ester group of the acrylic polymer with the hydroxyl-methyl group of chitosan (eq. 2-3, scheme 1). This conclusion is supported by the lack of the amide I band (within 1640-1680 cm^{-1}) and amide II band (within 1510-1580 cm^{-1}), which are associated with the C=O stretching vibration and in-plane



Scheme 1

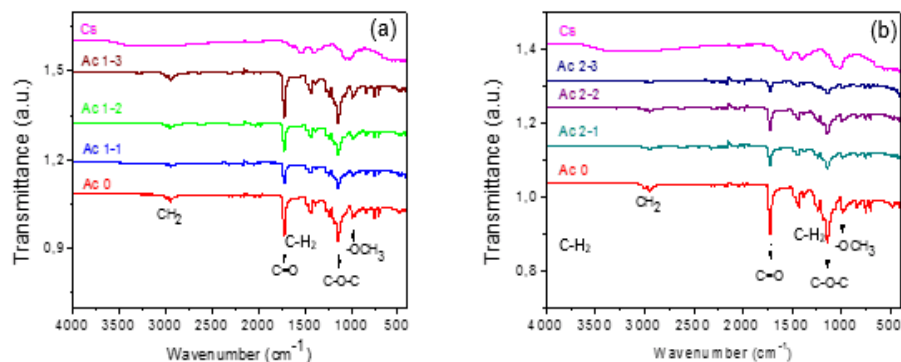


Fig. 1. ATR FTIR spectra of acrylic resin matrix (Ac0) sample and obtained hybrid materials: Ac1-1 to Ac 1-3 first series (a), and Ac 2-1 to Ac 2-3 second series (b)

N-H bending and C-N stretching vibration [20]. An arguments in favor of a transesterification reaction can be related to the fact that in the spectrum of PMMA (sample Ac0) only the band located at 984 cm⁻¹ associated with methyl rocking vibrations of methoxy group (O-CH₃) and the band located at 2954 cm⁻¹ associated with the methylene (-CH₂-) group show some shifts after chitosan grafting. As such, the band at 984-986 cm⁻¹ is shifted at 992-993 cm⁻¹, while the band at 2954 cm⁻¹ is shifted at 2945-2946 cm⁻¹, thus indicating the occurrence of a transesterification reaction of the methoxy group in the acrylic polymer with the hydroxy-methylene group of chitosan (chemical equations 2 and 3, scheme 1). In the same time, the fact that the band position of the carbonyl group (C=O) in the acrylic moiety (1721-1723 cm⁻¹) is not significantly affected by chitosan grafting could be explain because the resulting compound is still an ester, which is formed by the replacement of -CO(OCH₃) with -CO(OR), where R is the residue of chitosan.

For the preparation of the two series of hybrid materials, both components (P and L) of Duracryl were mixed with chitosan in different ways. In the first series, the chitosan was added after mixing the acryl powder and liquid components, which led to the attachment of chitosan molecules on the outer surface of PMMA layer (fig. 2a). For the second series, the chitosan solution was first mixed with Duracryl powder and then the Duracryl liquid component was added, leading to the chitosan attachment onto the surface of MMA-co-MA microspheres, followed by their covering with the PMMA film (fig. 2b). Therefore, in the first case the chitosan molecules are bonded on the outer surface of the hybrid material (fig. 2a), while in the second case the chitosan molecules are most probably inside of the hybrid material (fig. 2b).

SEM images show some differences in the morphology of the samples of the two series of hybrid materials (fig. 3).

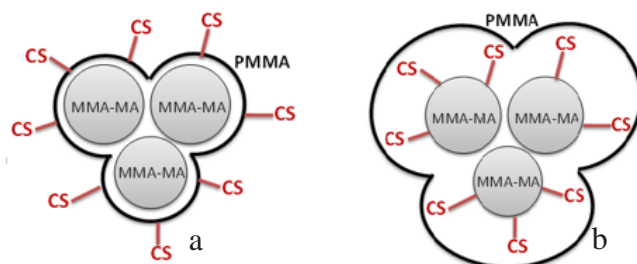


Fig. 2. Schematic representation of the structure of the first series (a) and second series (b) of hybrid materials obtained by adding chitosan to the commercial Duracryl product

First, one can note the compact arrangement of MMA-MA copolymer microspheres with consistent contact between them, within the un-grafted (Ac0) matrix. The MMA-MA microspheres are well connected to each other by wide bridges (fig. 3a). In the case of the samples of the first series, in which chitosan was added after mixing the Duracryl powder and liquid, it can be seen that the polymer film that surrounds the MMA-co-MA copolymer microspheres is not continuous and there is a higher porosity compared to that of samples without chitosan (Ac0) (fig. 3b).

The morphology of the second series of hybrid samples (fig. 3c) that were prepared by mixing the microspheres of Duracryl powder with chitosan followed by the addition of the liquid component (MMA), show that the MMA-co-MA microspheres are well embedded into a polymer matrix. The embedding matrix and the bridges between the microspheres show less pores and have a lower roughness (fig. 3c). The second sample from the second series with a lower content of chitosan (Ac2-3, fig. 3d) has a morphology very similar to the un-grafted acrylic matrix (fig. 3a).

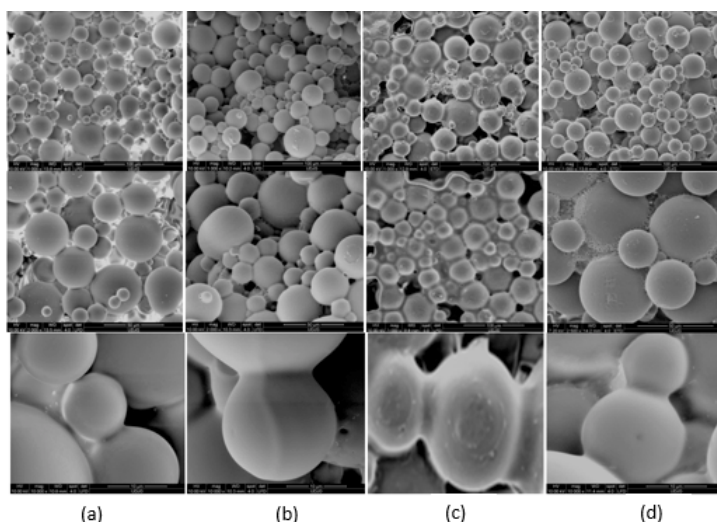


Fig. 3. SEM images on the surface of acrylic resin matrix-Ac0 sample (a) and the resulted hybrid materials with the same composition, but after different order of mixing, Ac1-2 (b) and Ac2-2 (c), and with different composition, Ac2-3 (d).

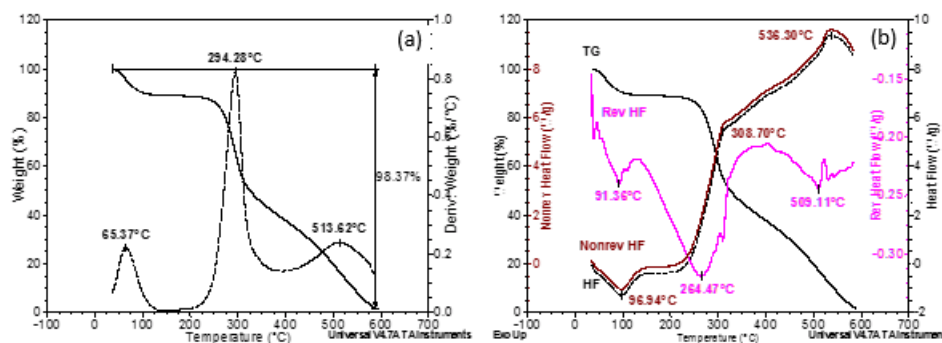


Fig. 4. mTG and mDTG curves (a) and the separation of total heat flow (HF) from the mDSC analysis in reversible (rev HF) and non-reversible (non-rev HF) heat flows (b) for chitosan thermal decomposition

Thermal behaviour and kinetic aspects

The mTG-mDTG curves of chitosan recorded in synthetic air (fig. 4) show three stages of decomposition. One can assume that the first step, from 50 to about 130 °C, can be attributed to the elimination of the adsorbed or chemisorbed water and amino groups, while the next two steps at 200-350°C and 400-600°C temperatures are attributed to the oxidative decomposition. The modulated DSC technique, by separation of total heat flow (HF) in reversible heat flow (revHF) associated with physical transformations and non-reversible heat flow (non-revHF) associated with chemical transformations, allows to observe that during all the three decomposition steps of chitosan in air, chemical and physical processes overlapped (fig. 4b). Thus, we can assume that between 50 and 130 °C there is an overlapping of the endothermic evaporation of water with the endothermic chemical breaking of hydroxyl groups from the C3 and C6 carbons or NH₂ groups of chitosan [8, 16]. In the second decomposition step (200-350°C) it can be seen an endothermic physical process (revHF peak) associated with exothermic chemical process (non-revHF peak), which may be explained by the elimination of the acetyl groups and/or depolymerization of chitosan [5] associated with air oxidation processes, respectively. This can explain why the TG-DTG curves for the decomposition of chitosan in nitrogen look quite similar with the curves of decomposition in synthetic air atmosphere [21].

The mTGA-mDTG-mDSC curves of the PMMA-based matrix together with the chitosan-grafted hybrid samples are shown in figures 5 and 6. The PMMA-based matrix (Ac0) shows the main decomposition process (more than 90% mass loss) between 300 and 400°C, with two endothermic peaks at 320 and 360 °C. In the case of the hybrid samples from the first series (table 1), the DTG curves show in the range 250-400°C an overlapping of two decomposition processes with peaks at about 290 and 360 °C (fig. 5b). The two peaks can be associated with the decomposition of chitosan (fig. 4a) and PMMA matrix (Ac0 sample in fig. 5b), respectively. The temperature of these peaks and the ratio of their intensity vary consistently with the ratio and order of mixing of chitosan and Duracryl liquid component (table 1). Unlike PMMA (Ac0), for which both peaks (320 and 360°C) are endothermic, for the hybrid samples one can firstly notice a drastic decrease in the intensity of the endothermic peaks and a shift of about 50 °C at higher temperature, and secondly, some new exothermic decomposition peaks related to the chitosan decomposition, as mentioned above.

As far as the hybrid samples of the second series are concerned, only for Ac2-3 sample, in which equal volumes of chitosan solution and liquid Duracryl representing each half of the volume of liquid used in Ac0 sample were added, the mDTG curve (fig. 6b) shows

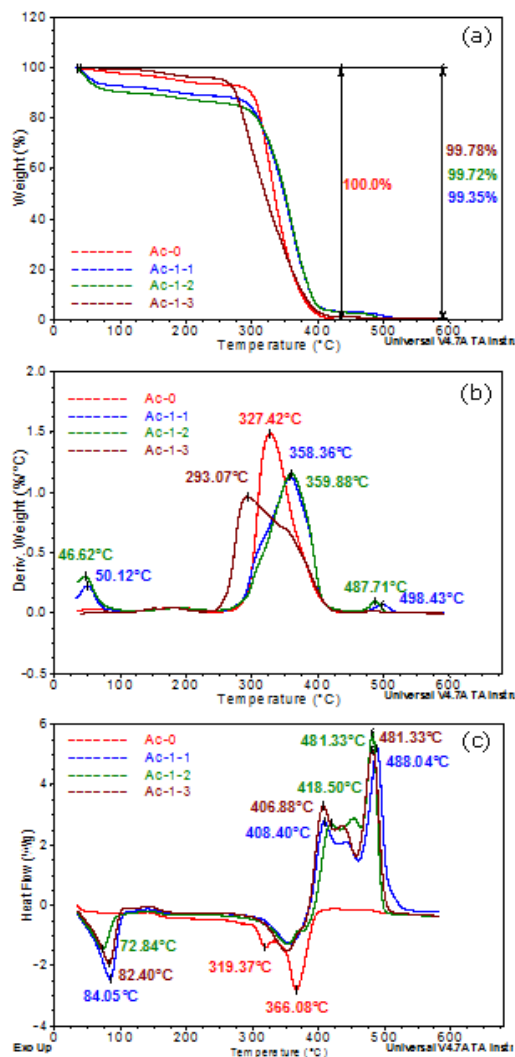


Fig. 5. mTGA (a), mDTG (b) and mDSC (c) curves of samples acrylic matrix (Ac0) and the hybrid samples from the first series (table 1)

two peaks at 296 and 353 °C, related to the decomposition of chitosan and PMMA, respectively. For the other two samples of this series, only the second peak of PMMA at 360 °C is observed (fig. 6b). Regarding the mDSC curves of the samples of the second series (fig. 6b) in which the Duracryl powder was added to the chitosan solution before mixing the liquid, they have a similar shape with the curves corresponding to the samples of the first series (fig. 5c). This indicates the same processes involved in the samples decomposition, but with different importance. In general, it can be concluded that grafting chitosan on the PMMA matrix significantly influences the thermal decomposition of each of them, indicating strong chemical grafting of chitosan to the polymer matrix, in agreement with the FTIR spectra.

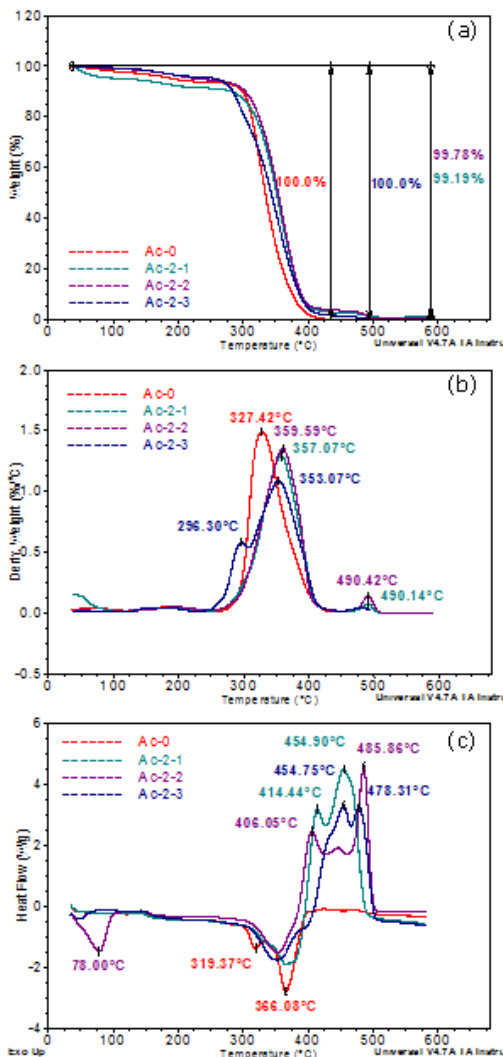


Fig. 6. mTGA (a), mDTG (b) and mDSC (c) curves of acrylic matrix (Ac0) sample and the hybrid samples from the first series (table 1)

Figure 7 shows the total (HF), reversible (revHF) and non-reversible (non-revHF) heat flow for the decomposition of Ac1-1 and Ac2-1 hybrid samples with the same composition, but different order of reagents mixing (series 1 and 2 in table 1). These curves indicate common features, but also highlight some differences. Thus, all three curves for both types of samples indicate an approximate overlapping of physical and chemical processes in the range 300-400 °C and a perfect overlapping of an exothermic chemical process with an endothermic physical one in the range 500-600 °C. The differences between the two types of samples consist in that for the Ac1-1 sample the three curves indicate an overlapping of endothermic physical and chemical processes at around 84 °C associated with slight weight loss (fig. 5a-b) and a gap between the endothermic non-reversible and reversible chemical processes (that succeed the non-reversible process) at 395 °C. Concerning sample Ac 2-1, there is no relevant physical or chemical process around 100 °C, the last two peaks are shifted to lower temperature (363.8 and 464 °C) and the ratio of their peaks intensity is different with respect to that of sample Ac1-1.

Usually, the data provided by the thermogravimetric analysis (TGA) are used to evaluate the kinetics of a weight loss process, by nonisothermal kinetic methods, like Flynn and Wall method [22]. Such methods need at least three experiments recorded at three different heating rates. In contrast to normal nonisothermal methods based on normal TGA data, the modulated thermogravimetric technique enables to obtain the kinetic parameters in a single nonisothermal experiment [23].

Figure 8a shows the values of the activation energy versus temperature, obtained from mTGA raw data of the thermal decomposition of the hybrid samples Ac1-1 and Ac2-1 (table 1). When there is no weight loss, the values of the activation energy are set at zero. The calculation of the activation energy is initiated once the weight loss process starts and, for a single-reaction mechanism, the activation energy should be a constant value during the whole weight loss region. At the beginning and the end of the weight loss region, the kinetic parameters go to unrealistically high values due to lack of reaction of material (weight loss).

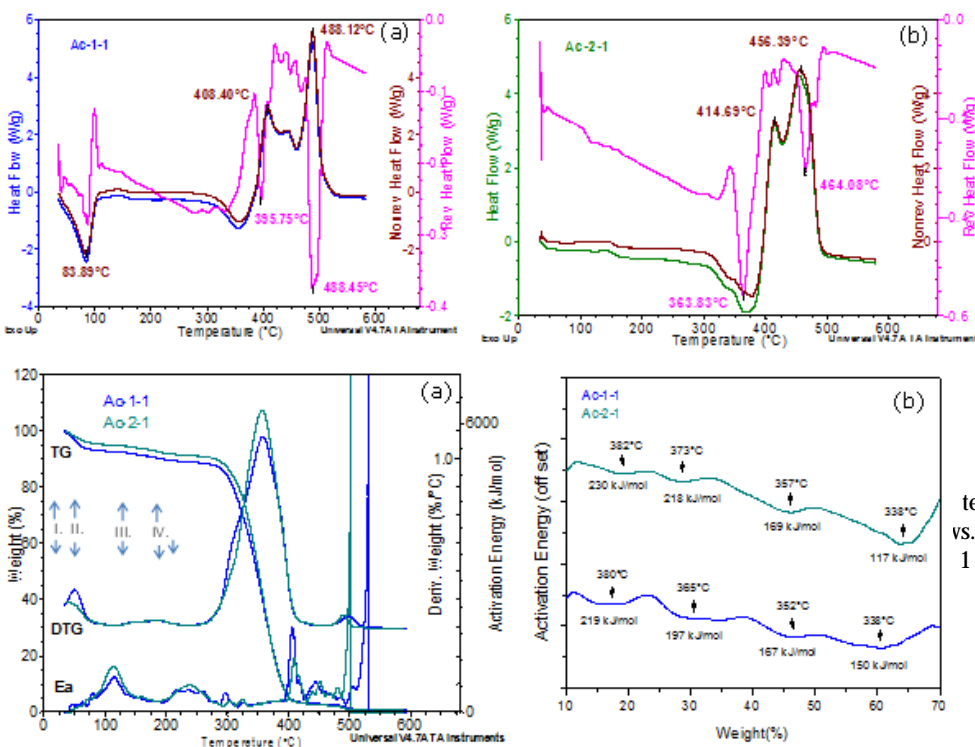


Fig. 7. Comparative mDSC results: total-HF, non-reversible-HF and reversible-HF curves for Ac1-1 (a) and Ac2-1(b) samples

Fig. 8. Comparative TGA-DTG-Ea vs. temperature (a) and corresponding Ea vs. sample weight (b) for Ac1-1 and Ac2-1 samples, corresponding to step IV in figure 8a

The peaks between the flat (constant) energy domains show the region of transition between the consecutive weight losses steps (steps I –II within 120-200°C and III - IV within 300-400°C ranges in fig. 8a). By plotting the activation energy as a function of weight percent, the variation of the activation energy versus the sample weight (degree of conversion) can be observed. This variation better highlights the effect of order of mixing between chitosan and the solid and liquid components of Duracryl upon the thermal decomposition of the obtained hybrid materials (fig. 8b). The curves of the samples Ac1-2 and Ac2-1 in figure 8b slightly change with the conversion degree, during the nonisothermal decomposition between 320 and about 400°C. The gradual slope of the curves show an activation energy changing with conversion, similar to the autocatalytic reactions [23].

Conclusions

The paper present some preliminary result on the thermal behavior, morphology and structure of some hybrid materials based on self-curing acrylic dental resin (Duracryl® Plus) modified with chitosan.

The grafting of chitosan on the acrylic resin takes place either on the surface of MMA-co-MA spheres of acrylic powder when chitosan was added before mixing the acrylic components (Series 1) or on the exterior PMMA polymer layer when the acrylic powder was first mixed with chitosan (Series 2). The results could suggest that in the conditions of our study the grafting of chitosan on the acrylic resin took place by transesterification reaction between the ester group of the acrylic polymer and the hydroxyl-methyl group of chitosan.

There are three steps of thermal decomposition in air of the obtained hybrid materials between 25 and 600 °C. For both types of samples belonging to the two series, there is an overlapping of physical and chemical decomposition processes in the range 300-400 °C and an overlapping of the exothermic chemical oxidative decomposition process with an endothermic physical one in the range 500-600 °C. The two types of samples have a different behavior in the range of 25-100 °C, namely, opposed to the samples from the first series, the samples from the second series do not show endothermic processes with mass loss below 100 °C.

The activation energy of the decomposition between 320 and 380 °C (main decomposition step with about 90% mass loss) changes its value from 117 to 230 kJ/mol (Series 1) and from 150 to 380 kJ/mol (Series 2) with the conversion degree, similar to autocatalytic reactions.

The study will be continued to better highlight the chemical interactions between chitosan and acrylic polymers and to optimize the properties of hybrid material depending on the conditions of preparation.

Acknowledgement: The authors acknowledge the support provided by the Project Romanian center for modeling the aquaculture recirculating systems, ID 1815, co-financed by the European Regional Development Fund through the Operational Programme Increase Economic Competitiveness, Axis 2 POSCCE, O2.2.1 and Prof. PhD Rodica Dinica and PhD Aurel Tabacaru for ATR-FTIR spectra and their interpretation.

References

1. ELIZALDE-PENA, E.A., FLORES-RAMIREZ, N., LUNA-BARCENAS, G., VIQUEZ-GARCIA, S.R., ARIEMBULA-VILLA, G., GARCIA-GAITLN, B., RUTIAGA-QUINONES, J.G., GONZALEZ-HERNANDEZ, J., *Eur. Polym. J.*, **43**, 2007, p. 3963-3969
2. <http://plastics.ulprospector.com/generics/3/c/t/acrylic-properties-processing>
3. ZHANG, X., ZHANG, X., ZHU, B., LIN, K., CHANG, J., *Dent. Mater. J.*, **31**, nr. 6, 2012, p. 903-908
4. SPASOJEVIC, P., ZRLIC, M., PANIC, V., STAMENKOVIC, D., SESLIJA, S., VELICKOVIC, S., *Int. J. Polym. Sci.*, 9 pages, 2015, <http://dx.doi.org/10.1155/2015/561012>
5. PATI, M.K., NAYAK, P., *Mat. Sci. Appl.*, **2**, 2011, p.1741-1748
6. CAVALU, S., SIMON, V., GOLLER, G., AKIN, I., *Digest J. Nanomat. Biostruct.*, **6**, nr. 2, 2011, p. 779-790
7. NATHIYA, S., DURGA, M., DEVASENA, T., *Digest J. Nanomat. Biostruct.*, **9**, nr. 4, 2014, p. 1603- 1614
8. LIU, X., MA, L., MAO, Z., GAO, C., *Adv. Polym. Sci.*, **244**, 2011, p. 81-128
9. ZECHERU, T., ZAHARIA, C., SALAGEANU, A., TUCUREANU, C., RUSEN, E., MARCULESCU, B., ROTARIU, R., CINCU, C., *Journal of Optoelectronics and Advanced Materials*, 9, no. 9, 2007, p. 2917
10. RUSEN, E., MARCULESCU, B., BUTAC, L., ZECHERU, T., MICULESCU, E., ROTARIU, T., *Journal of Optoelectronics and Advanced Materilas*, 10, no. 12, 2008, p. 3436
11. SANFORD, P.A., chapter: Chitosan—commercial uses and potential applications, Chitin and Chitosan, G. Skjak-Braeck, T. Anthonsen, and P.A. Sandford, Eds., Elsevier, London, 1989, p. 51-70
12. MUZZARELLI, R.A.A., *Cell Mol. Life Sci.*, **53**, 1997, p. 131-140
13. FELT, O., BURI, P., GURNY, R., *Drug Dev. Ind. Pharm.*, **24**, 1998, p. 979-993
14. LUO, G., SAMARANAYAKE, L.P., *Acta Pathol. Microb. Immun. Scand. (APMIS)*, **110**, nr. 9, 2002, p. 601-10
- 15.*** <http://www.spoofadental.com/EN/products/dental-resins/denture-base-resins/duracryl-plus/productfamily/DuracrylPlus>
16. JALAL ZOHURIAAN-MEHR, M., *Iranian Polym. J.*, **14**, nr. 3, 2005, p. 235-265
17. JIANG, J., GAO, D., LI, Z., SU, G., *React. Funct. Polym.*, **66**, 2006, p. 1141-1148
18. NAYAK, P.L., *J. Macromol. Sci. Rev. Macromol. Chem. Phys.*, **14**, 1996, p. 193-213
19. HEDZELEK, W., WACHOWIAK, R., MARCINKOWSKA, A., DOMKA, L., *Acta Phys. Pol.*, **114**, nr. 2, 2008, p. 471-484
20. HARISH PRASHANTH, K.V., THARANATHAN, R.N., *Carbohydr. Polym.*, **54**, 2003, p. 343-351
21. WILKIE, C.A., *Polym. Degrad. Stabil.*, **66**, 1999, p. 301-306
22. FLYNN, J.H., WALL, L.A., *Polym. Lett.*, **4**, 1996, p. 323-328
23. BLAINE, R., *Amer. Lab.*, **30**, nr. 1, 1998, p. 21

Manuscript received: 2.02.2016